

Structure and stability of copper clusters : A tight-binding molecular dynamics study

Mukul Kabir and Abhijit Mukherjee^y
S.N. Bose National Centre for Basic Sciences, JD Block,
Sector III, Salt Lake City, Kolkata 700098, India

A.K. Bhattacharya
Department of Engineering, University of Warwick, Coventry CV47AL, U.K.
(Dated: April 17, 2024)

In this paper we propose a tight-binding molecular dynamics with parameters fitted to first-principles calculations on the smaller clusters and with an environment correction, to be a powerful technique for studying large transition/noble metal clusters. In particular, the structure and stability of Cu_n clusters for $n = 3 - 55$ are studied by using this technique. The results for small Cu_n clusters ($n = 3 - 9$) show good agreement with ab initio calculations and available experimental results. In the size range $10 \leq n \leq 55$ most of the clusters adopt icosahedral structure which can be derived from the 13-atom icosahedron, the polyicosahedral 19-, 23-, and 26-atom clusters and the 55-atom icosahedron, by adding or removing atoms. However, a local geometrical change from icosahedral to decahedral structure is observed for $n = 40 - 44$ and return to the icosahedral growth pattern is found at $n = 45$ which continues. Electronic "magic numbers" ($n = 2, 8, 20, 34, 40$) in this regime are correctly reproduced. Due to electron pairing in HOMOs, even-odd alternation is found. A sudden loss of even-odd alternation in second difference of cluster binding energy, HOMO-LUMO gap energy and ionization potential is observed in the region $n \geq 40$ due to structural change there. Interplay between electronic and geometrical structure is found.

PACS numbers: 36.40.-c, 36.40.Cg, 36.40.Mr, 36.40.Qv

I. INTRODUCTION

The study of clusters has become an increasingly interesting topic of research in both physics and chemistry in recent years, since they span the gap between the microscopic and macroscopic materials [1, 2]. Metallic clusters play a central role in catalysis [3, 4, 5, 6] and nanotechnology [7, 8, 9]. Clusters of coinage metals Cu, Ag and Au have been used in a wide range of demonstration [3, 4, 5, 6, 7, 8, 9]. The determination of structural and electronic properties and the growth pattern of coinage metal clusters are of much interest both experimentally [10, 11, 12, 13, 14, 15, 16, 17, 18] and theoretically [19, 20, 21, 22, 23, 24]. The electronic configuration of the coinage metals are characterized by a closed d shell and a single s valence electron [$Cu: Ar(3d)^{10}(4s)^1$, $Ag: Kr(4d)^{10}(5s)^1$, $Au: Xe(5d)^{10}(6s)^1$]. Due to the presence of single s electrons in the atomic outer shells, the noble metal clusters are expected to exhibit certain similarities to the alkali metal clusters. Electronic structure of alkali metal clusters are well described by the spherical shell model, which has successfully interpreted the "magic numbers" in Na_n and K_n clusters [1, 2]. A number of experimental features of noble metal clusters are also qualitatively well described in terms of simple s electron shell model. For instance, the mass abundance

spectrum of Cu_n , Ag_n and Au_n clusters, which reflects the stability of clusters, can be explained by the one-electron shell model [10]. But some experimental studies [11, 12, 13, 14] indicate that the localized d electrons of the noble metals play a significant role for the geometrical and electronic structure through the hybridization with more extended valence s electron. Therefore, it is important to include the contribution of 3d electrons and the s-d hybridization for Cu_n clusters.

Bare copper clusters in the gas phase have been studied experimentally by Taylor et al. [15] and Ho et al. [16] using photoelectron spectroscopy (PES). Nickel-beam measured ionization potentials of neutral copper clusters and found evidence of electronic shell structure [17]. Very recently cationic copper clusters have been studied using threshold collision-induced dissociation (TCID) by Spasov et al. [18]. Copper clusters have been also investigated theoretically by various accurate quantum mechanical and chemical approaches. Massobrio et al. [19] studied the structures and energetics of Cu_n ($n = 2; 3; 4; 6; 8; 10$) within the local density approximation of density functional theory (DF-LDA) by using the Car-Parinello (CP) method. Calaminci et al. [20] used the linear combination of Gaussian-type orbitals density functional (LCGTO-DFT) approach to study Cu_n , Cu_n^- and Cu_n^+ clusters with $n \leq 5$. Akeby et al. [21] used the configuration interaction (CI) method with an effective core potential (ECP) for $n \leq 10$. In an earlier communication [22] we studied the small Cu_n clusters for $n \leq 9$ by using full-potential mu n-tin orbitals (FP-LMTO) technique.

^yMailing author's e-mail address: mukul@bose.res.in
e-mail address: abhijit@bose.res.in

Ideally, the sophisticated, quantum chemistry based, first-principles methods predict both the stable geometries and energetics to a very high degree of accuracy. The practical problem arises from the fact that for actual implementation these techniques are limited to small clusters only. None of the methods described above can be implemented for clusters much larger than 10 atoms, because of prohibitive computational expense. The aim of this communication is to introduce an semi-empirical method, which nevertheless retains some of the electronic structure features of the problem. The empirical parameters are determined from first-principles calculations for small clusters, and corrections introduced for local environmental corrections in the larger clusters.

In recent years empirical tight-binding molecular dynamics (TBMD) method has been developed as an alternative to ab initio methods. As compared with ab initio methods, the parameterized tight-binding Hamiltonian reduces the computational cost dramatically. The main problem with the empirical tight-binding methods has always been the lack of transferability of its empirical parameters. We shall describe here a technique that allows us to fit the parameters of the model from a fully ab initio, self-consistent local spin-density approximation (LSDA) based FP-LMTO calculation reported earlier by us [22, 23] for the smaller clusters and then make correction for the new environment for clusters in order to ensure transferability (at least to a degree).

It should be mentioned here that Copper clusters have also been investigated by other empirical methods. D'Astino carried molecular dynamics using a quasi-empirical potential derived from a tight-binding approach for nearly 1300 atoms [24]. More recently Darby et al. carried geometry optimization by genetic algorithm using Gupta potential [25] for Cu_n , Au_n and their alloy clusters in the size range $n \leq 56$ [26]. These kinds of empirical atomistic potentials are found to be good to predict ground state geometries but can not predict electronic properties such as electronic shell closing effect for $n = 2, 8, 20, 40, \dots$, highest occupied-lowest unoccupied molecular level (HOMO-LUMO) gap energy and ionization potential. Our proposed TBMD scheme will allow us to extrapolate to the larger clusters to study both the ground state geometries as well as ground state energetics as a function of cluster size.

Menon et al. have proposed a minimal parameter tight-binding molecular dynamics (TBMD) scheme for semiconductors [27, 28, 29] and extended the method for transition metal (N_n and Fe_n) clusters [30, 31]. Recently Zhao et al. has applied this method for silver clusters [32]. In the present work, we shall introduce a similar TB model for copper.

Using this TBMD method, we shall investigate the stable structures, cohesive energies, relative stabilities, HOMO-LUMO gaps and ionization potentials of Cu_n clusters in the size range $n \leq 55$. We shall indicate the comparison between the present results for small clusters, $n \leq 9$, with those of our previous FP-LMTO calculations

and other ab initio and available experimental results. This is essential before we go over to the computationally expensive study of larger clusters.

II. COMPUTATIONAL METHOD

Menon et al. introduced a minimal parameter tight-binding molecular dynamics (TBMD) scheme for transition metal clusters [30, 31]. Here we will describe the main ingredients. In this tight-binding scheme the total energy E is written as a sum,

$$E = E_{el} + E_{rep} + E_{bond}; \quad (1)$$

E_{el} is the sum of the one-electron energies for the occupied states k ,

$$E_{el} = \sum_k \epsilon_k^{occ}; \quad (2)$$

where the energy eigenvalues ϵ_k are calculated by solving the eigenvalue equation

$$H j_k i = \epsilon_k j_k i; \quad (3)$$

where H is the one-electron Hamiltonian and $j_k i$ is electronic wave function for k th level of the eigenstate. In the TB formulation, the single particle wavefunctions $j_k i$ are cast as a linear combination of orthogonalized basis functions i , in the minimum basis set ($i = s; p_x; p_y; p_z; d_{xy}; d_{yz}; d_{zx}; d_{x^2-y^2}; d_{3z^2-r^2}$),

$$j_k i = \sum_i c_i^k j_i i; \quad (4)$$

where i labels the ions.

The TB Hamiltonian H is constructed within Slater-Koster scheme [33], where the diagonal matrix elements are taken to be configuration independent and the off-diagonal matrix elements are taken to have Slater-Koster type angular dependence with respect to the inter-atomic separation vector r and scaled exponentially with the inter-atomic separation r :

$$V_{l;m;n}(\mathbf{r}) = V_{l;m;n}(d) S(l;m;n) \exp[-\alpha(r-d)]; \quad (5)$$

where d is the equilibrium bond length for the fcc bulk copper, $S(l;m;n)$ is the Slater-Koster type function of the direction cosines $l;m;n$ of the separation vector r and α is an adjustable parameter ($\alpha = 2/d$) [31].

The Hamiltonian parameters are determined from the dimensionless universal parameters $\epsilon_{s;s}, \epsilon_{s;p}, \epsilon_{p;p}$ [34],

$$V_{l;m;n}(\mathbf{r}) = \epsilon_{l;m;n} \frac{r_d^2}{m d^{l+m+n+2}}; \quad (6)$$

where r_d is characteristic length for the transition metal and the parameter $\epsilon_{l;m;n} = 0$ for $s-s, s-p$ and $p-p$ interactions, $\epsilon_{l;m;n} = 3/2$ for $s-d$ and $p-d$ interactions and $\epsilon_{l;m;n} = 3$

TABLE I: Parameter r_d , on-site energies E_s , E_p and E_d and the universal constants ϵ_0 , ϵ_∞ for Cu [34].

Parameter	Value	Parameter	Value
r_d	0.67 Å	pp	-0.81
E_s	-20.14 eV	sd	-3.16
E_p	100.00 eV	pd	-2.95
E_d	-20.14 eV	pd	1.36
ss	-0.48	dd	-16.20
sp	1.84	dd	8.75
pp	3.24	dd	0.00

for d-d interaction. In Table I we present the parameter r_d , the on-site energies E_s , E_p , E_d and the universal constants ϵ_0 , ϵ_∞ for Cu [34]. According to Ref.[30] and Ref.[31], we set $E_s = E_d$ and E_p large enough to prevent p-orbital mixing [34]. This choice of our tight-binding parameters reproduces the band structure of the fcc bulk Cu crystal given by Harrison [34].

The repulsive energy E_{rep} is described by a sum of short-ranged repulsive pair potentials, v_{ij} , which scaled exponentially with inter-atomic distance,

$$E_{rep} = \sum_{i,j} \sum_{i,j > i} v_{ij}(r_{ij}) = \sum_{i,j > i} \epsilon_0 \exp[-(r_{ij} - d)]; \quad (7)$$

where r_{ij} is the separation between the atom i and j and $(= 4)$ is a parameter. E_{rep} contains ion-ion repulsive interaction and correction to the double counting of the electron-electron repulsion present in E_{el} . The value of ϵ_0 is fitted to reproduce the correct experimental bond length of the Cu dimer 2.22 Å [35] is given in Table II.

The first two terms of the total energy are not sufficient to exactly reproduce cohesive energies of dimers through bulk structures. Tománek and Schlüter [36] introduced a coordination dependent correction term, E_{bond} , to the total energy, which does not contribute to the force, it is added to the total energy after the relaxation has been achieved. However, for the metal clusters, this correction term is significant in distinguishing various isomers for a given cluster [31].

$$E_{bond} = n_a \frac{n_b^2}{n} + b \frac{n_b}{n} + c; \quad (8)$$

where n and n_b are the number of atoms and total number of bonds of the cluster respectively. Number of bonds n_b are evaluated by summing over all bonds according to cut-off distance r_c and bond length

$$n_b = \sum_i \exp \left[\frac{r_{ij} - r_c}{4} \right] + 1; \quad (9)$$

The parameters a , b and c in the equation (6) are then calculated by fitting the coordination dependent term,

TABLE II: The adjustable parameters ϵ_0 , a , b ; and c .

ϵ_0 (eV)	a (eV)	b (eV)	c (eV)
0.034	-0.0671	1.2375	-3.0420

E_{bond} , to the ab initio results for three small clusters of different sizes according to the following equation

$$E_{bond} = E_{ab initio} - E_{el} - E_{rep}; \quad (10)$$

Thus we have four parameters ϵ_0 , a , b , and c in this TB model. These parameters are once calculated (given in the Table II) for small clusters to reproduce known results (whatever experimental or theoretical) and then kept fixed for other arbitrary size cluster. To determine the parameters a , b and c we use the experimental binding energy of Cu dimer 1.03 eV/atom [35] and the ab initio FP-LMTO results for Cu_4 and Cu_6 in Ref. [22]. For the Cu_2 dimer calculated vibrational frequency (226 cm^{-1}) has reasonable agreement with experiment [37] (265 cm^{-1}).

In molecular dynamics scheme the trajectories $\mathbf{r}_j(t)$ of the ions are determined by the potential energy surface $E[\mathbf{r}_j(t)]$ corresponding to the total energy of the electronic system. The force acting on the i -th ion is thus given by,

$$\mathbf{F}_i = -\nabla_{\mathbf{r}_i} E_{el}[\mathbf{r}_j] - \nabla_{\mathbf{r}_i} E_{rep} = -\nabla_{\mathbf{r}_i} \sum_k \mathbf{h}_k \mathbf{H}_j \mathbf{h}_k + E_{rep} \quad (11)$$

This equation can be further simplified by making use of the Hellmann-Feynman [38] theorem

$$\mathbf{F}_i = -\sum_k \nabla_{\mathbf{r}_i} \mathbf{h}_k \mathbf{H}_k \mathbf{h}_k - \nabla_{\mathbf{r}_i} E_{rep}; \quad (12)$$

The second term in the above equation is the short-ranged repulsive force. We should note that Pulay correction term does not play any role in any semi-empirical TBMD [39]. The reason is twofold. Within TBMD we directly compute the derivative of the TB Hamiltonian matrix element and the basis wavefunctions never appear explicitly, rather they are implicitly contained in the fitted matrix entries.

The motion of the atoms follow a classical behaviour and is governed by the Newton's law:

$$m \frac{d^2 \mathbf{r}_i}{dt^2} = \mathbf{F}_i; \quad (13)$$

where m is the atomic mass.

For numerical simulation of Newtonian dynamics, we use the velocity Verlet molecular dynamics method [40] for updating the atomic coordinates, which is given by,

$$\mathbf{r}_i(t + \Delta t) = \mathbf{r}_i(t) + \mathbf{V}_i(t) \Delta t + \frac{1}{2m} \mathbf{F}_i(t) (\Delta t)^2; \quad (14)$$

TABLE III: Point group (PG) symmetry, cohesive energy per atom, difference in cohesive energy per atom ΔE and average bond length $\langle r \rangle$ of the ground state structure and different isomers for Cu_n clusters with $n \leq 9$ obtained from TB calculation and comparison with ab initio calculations [19, 21, 22]. $\Delta E = 0.00$ represents the most stable structure for a particular n . Cohesive energy corresponding to the ground state structure in FP-LMTO [22], DF-LDA [19] (in parentheses) calculations and the values from TCID experiment [18] are given. For Cu_7 , $C_{3v}(I)$ is the bicapped trigonal bipyramid and $C_{3v}(II)$ is the capped octahedron.

Cluster	PG Symmetry	Binding Energy (eV/atom)			ΔE (eV/atom)			$\langle r \rangle$ (Å)
		Present	Theory ^a	Experiment ^b	Present	Theory ^c	Theory ^d	
Cu_3	C_{2v}	1.43	1.60 (1.63)	1.07 ± 0.12	0.00		0.00	2.25
	D_{3h}	1.32			0.11	0.06		2.24
	D_{1h}	1.13			0.30	0.00		2.24
Cu_4	D_{2h}	2.00	2.00 (2.09)	1.48 ± 0.14	0.00	0.00	0.00	2.23
	D_{4h}	1.73			0.27	0.56		2.22
	T_d	1.46			0.54	0.89		2.24
Cu_5	C_{2v}	2.24	2.19	1.56 ± 0.15	0.00	0.00		2.23
	D_{3h}	2.03			0.21	0.37		2.38
Cu_6	C_{5v}	2.54	2.40 (2.49)	1.73 ± 0.18	0.00	0.00	0.00	2.40
	C_{2v}	2.40			0.14		0.01	2.39
	O_h	1.98			0.56	0.87	0.04	2.41
Cu_7	D_{5h}	2.63	2.65	1.86 ± 0.22	0.00	0.00		2.41
	$C_{3v}(I)$	2.50			0.13	0.32		2.63
	$C_{3v}(II)$	2.30			0.33			2.45
Cu_8	C_s	2.87	2.73 (2.84)	2.00 ± 0.23	0.00		0.20	2.41
	O_h	2.64			0.23			2.61
	D_{2d}	2.57			0.30		0.00	2.59
	T_d	2.51			0.36		0.15	2.39
Cu_9	C_2	2.87	2.80		0.00			2.44
	C_{2v}	2.84			0.03			2.59
	C_s	2.60			0.27			2.41

^aFrom Kabir et al. (Ref.[22]) and Massobrio et al. (Ref.[19]).

^bCalculated from Spasov et al. (Ref.[18]).

^cFrom Akeby et al. (Ref.[21]).

^dFrom Massobrio et al. (Ref.[19]).

where the velocity V_i of the i th atom at $t + \Delta t$ is calculated from F_i at t and $t + \Delta t$ as

$$V_i(t + \Delta t) = V_i(t) + \frac{1}{2m} [F_i(t) + F_i(t + \Delta t)] \Delta t \quad (15)$$

At this stage most authors carry out either dissipative dynamics or free dynamics with feedback [41]. The reason for this is as follows: for numerical integration of Newton's equations we have to choose a finite time step Δt . Ideally this should be as small as possible, but that would require an excessively long time for locating the global minimum. However, a large choice of Δt leads to unphysical heating up of the system, leading to instability. Dissipative dynamics has been suggested as a way of overcoming this. We add a small extra friction term carefully $F \rightarrow F - \gamma m \dot{R}$ [31]. In the present calculation $\gamma = 0.32$ amu/psec, and the time step Δt is taken to be 1 fsec and the total time for molecular dynamics simulation is 100–200 psec, depending upon the cluster size and initial cluster configuration with the several annealing schedule. Methfessel and Schilfgaarde [41] have also used an alternative technique of free dynamics with feedback to overcome the above difficulty.

The results of the molecular dynamics may depend sensitively on the starting configuration chosen. The final

equilibrium configurations often correspond to local minima of the total energy surface and are metastable states. For the smaller clusters simulated annealing can lead to the global minimum. We have found the global minimum configurations of the smaller clusters by the simulated annealing technique. However, this is often not the case for the larger clusters. Recently more sophisticated techniques like the genetic algorithm has been proposed [42]–[45]. We have not tried this out in this communication, but propose this as an efficient technique for further work.

III. RESULTS AND DISCUSSION

A. Geometry optimization

We have applied this TBM D scheme to Cu_n clusters for $n \leq 55$. Since the present scheme imposes no a priori symmetry restrictions, we can perform full optimization of cluster geometries. For small clusters ($n \leq 9$) we can able to perform a full configurational space search to determine the lowest-energy configuration. Here they serve as a test case for the calculation of larger clusters with

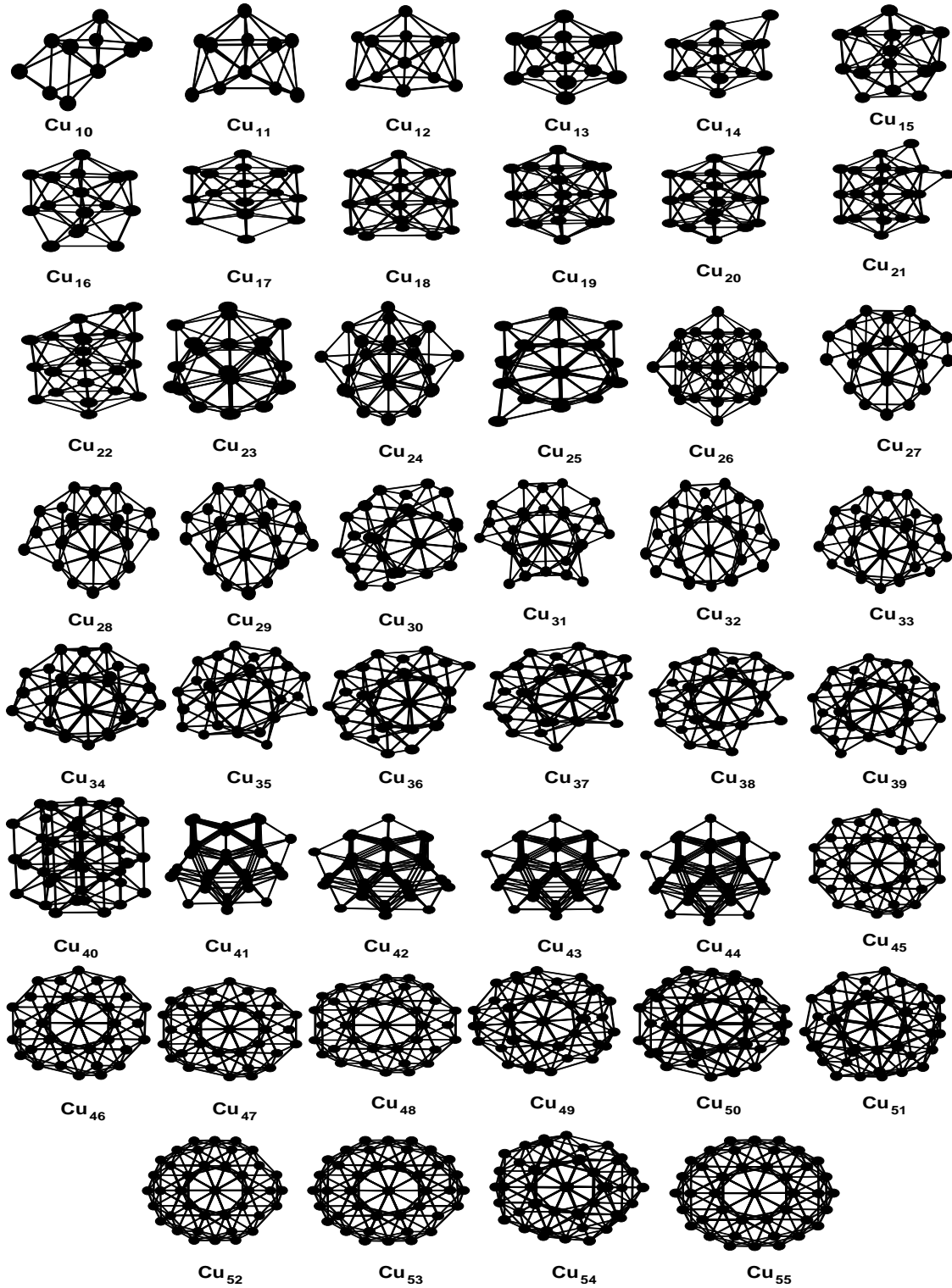


FIG. 1: Most stable structures for copper clusters with $n = 10$ –55 atoms. Most of the clusters adopt icosahedral structures except for $n = 40$ –44, where the structures are decahedral.

$n = 10$. In Table III we present a detailed comparison of binding energy per atom, difference in binding energy 4 eV and average bond length $\langle r \rangle$ for $n = 9$ with available experimental [18] and ab initio [19, 21, 22] results. We

found, in agreement with experimental [16] and theoretical [19, 20, 21] results, very small copper clusters (Cu_3 , Cu_4 and Cu_5) prefer planar structures. More detailed comparison, with experimental and ab initio results, can

be found elsewhere [46].

From the present results and detailed comparisons with various experimental [16, 18] and ab initio [19, 20, 21, 22, 47, 48, 49] results available, we find reasonable agreement among this TBM D scheme and ab initio calculations for small clusters with $n \leq 9$ [46], which allow us to continue the use of this TBM D scheme for larger clusters with $n \geq 10$. For larger clusters ($10 \leq n \leq 55$), due to increasing degrees of freedom with cluster size, a full conformational search is not possible with the available computational resources. Instead, led by the experimental and theoretical results on small clusters, we examined structures of various symmetries for each size. Most stable structures for $n = 10 - 55$ atom clusters are given in Fig.1.

In this regime, the structures predicted by this TBM model are mainly based on icosahedron. The most stable structure of Cu_7 is a pentagonal bipyramid (D_{5h} symmetry; see Table III), which is the building block for the larger clusters with $n \geq 10$. For Cu_{10} , we found a tricapped pentagonal bipyramid to be the most stable structure. Ground state structures of Cu_{11} and Cu_{12} are the uncompleted icosahedron with lack of one and two atoms respectively and a Jahn-Teller distorted first closed shell icosahedron is formed at Cu_{13} . For Cu_{13} , the fcc-like cuboctahedron is less stable than the icosahedron by an energy 0.05 eV per atom. In agreement Lammer and Borstel, on the basis of tight-binding linear muffin-tin orbital calculations, was also found the icosahedron to be the ground state of Cu_{13} , though the difference in energy between the icosahedron and the cuboctahedron was calculated to be only 0.2 eV/atom [48]. The ground state structures for Cu_{14} , Cu_{15} , Cu_{16} , and Cu_{17} are the 13-atom icosahedron plus one, two, three and four atoms respectively. A double icosahedron is formed for Cu_{19} (D_{5h} symmetry). This structure has two internal atoms, 12 six-coordinate atoms at either end and eight-coordinate atoms around the waist of the cluster. Based on the structure for Cu_{19} , the stable Cu_{18} cluster is a double icosahedron minus one of the six-coordinate atoms located at either end (C_{5v} symmetry). Icosahedral growth continues for $20 \leq n \leq 55$ atom clusters. Polyicosahedral structure in the form of a "triple icosahedron" (D_{3h} symmetry; the structure can be viewed as three interpenetrating double icosahedra) is the most stable structure for Cu_{23} cluster. The next closed shell polyicosahedra is found for Cu_{26} cluster. Finally, the second closed shell icosahedron is formed for Cu_{55} which is more stable than the closed cuboctahedral structure by an energy difference 6.27 eV. This can be explained in terms of their surface energy. The surface energy of the icosahedral structure is lower than that of the cuboctahedral structure, because the atoms on the surface of the icosahedron are five-coordinate compared to the four-coordinate atoms on the surface of the cuboctahedron. In our calculation, exception to the icosahedral growth is found at around Cu_{40} . The situation regarding geometrical structure in this size range is more

complex. The structures for $n = 40 - 44$ atom clusters are oblate, decahedron like geometries. Return to the icosahedral structure is found at $n = 45$. In the size range $n = 40 - 44$, the structural sequence is decahedron-icosahedron-cuboctahedron in decreasing order of stability, whereas in the region $n = 45 - 55$, the structures retain icosahedron-decahedron-cuboctahedron sequence.

This results are in agreement with the experimental study of Winter and co-workers [50], where they found a bare copper cluster mass spectrum recorded with ArF laser ionization shows a sudden decrease in the ion signal at Cu_{42}^+ , and from this observation they argued that a change in geometrical structure might occur there, though they have not concluded about the nature of this geometrical change. They also found a dramatic decrease in water binding energy for Cu_{50} and Cu_{51} , and concluded that this may represent a return to the icosahedral structure as the closed shell at Cu_{55} is approached.

D'Agostino [24] confirms our prediction, who performed molecular dynamics using a tight-binding many-body potential and found that icosahedral structures are prevalent for clusters containing less than about 1500 atoms. Valkealahti and Manninen [51], using effective medium theory, also found icosahedral structures are energetically more favourable than the cuboctahedral structures for sizes up to $n \leq 2500$ is consistent with our result: Fig.3 shows cuboctahedral structures are least stable among the three structures, icosahedron, decahedron and cuboctahedron. By contrast, Christensen and Jacobsen [52] predicted more fcc-like structures in the size range $n = 3 - 29$, in their Monte Carlo simulation using an effective medium potential. But they correctly reproduced the "magic numbers" in that regime [52, 53].

These results can be compared with the genetic algorithm study on copper clusters by Darby et al. [26], using Gupta potential. In agreement with the present study, Darby et al. found that most of the clusters in this regime adopt structures based on icosahedron. They also found exceptions to the icosahedral growth at around Cu_{40} , where the structures adopt decahedron like geometries (exact numbers are not available in the Ref. [26]). But the present study disagree with the genetic algorithm study in two points. Firstly, for 25 atom cluster, they found a more disordered structure, while the present study predict it to be an icosahedron based structure which can be derived by removing one surface atom from the 26-atom polyicosahedron. Finally, they found an fcc-like truncated octahedral structure for Cu_{38} . Instead, the present study predict the icosahedron based structure to be the ground state, where this structure is energetically more favourable than the truncated octahedral structure by an energy $4E = 0.17$ eV/atom. Although the genetic algorithm search for global minimum is more efficient technique than molecular dynamics, use of the empirical atomistic potential is the main reason [54] for this kind of disagreement between Darby et al. and the present study.

B. Binding energies and relative stabilities

The computed size dependence of the binding energy per atom for Cu_n clusters with $n = 2 - 55$ is depicted in Fig.2 (upper panel). Among all the isomeric geometries examined for a certain cluster size n , the highest cohesive energy has been considered for the Fig.2. The overall shape of the curve matches the anticipated trend: binding energy grows monotonically with increasing the cluster size. Inset of the Fig.2 (upper panel) shows the comparison of our calculated binding energy with the ab initio [19, 22] and experimental [18] results. Experimentally the binding energies of the neutral clusters were derived from the dissociation energy data of anionic clusters from the TCD experiment [18] and using electron affinities from the PES experiment [16]. The inset figure shows that our calculated binding energies are in good agreement with those from DF-LDA [19] and our previous FP-LMTO [22] calculations. However, our binding energies are systematically overestimated, by an energy 0.53 - 0.12 to 0.79 - 0.22, than the experimental bind-

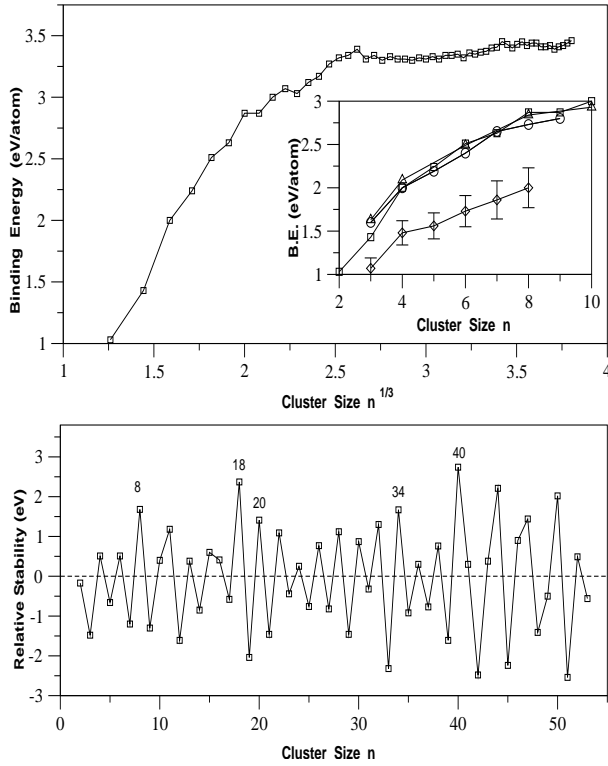


FIG. 2: (Upper panel) Binding energy per atom as a function of cluster size $n^{1/3}$. Inset of the upper panel represents a comparison of binding energy per atom as a function of cluster size n , among the present TBMD (○), FP-LMTO (□), DF-LDA (△) calculations and experimental (●) values. (Lower panel) Variation of relative stability 4_2E with cluster size n . Shell closing effect at $n = 8; 18; 20; 34; 40$ and even-odd alternation up to $n = 40$ are found. However, due to geometrical effect this even-odd alternation is disturbed at $n = 11; 13$ and 15.

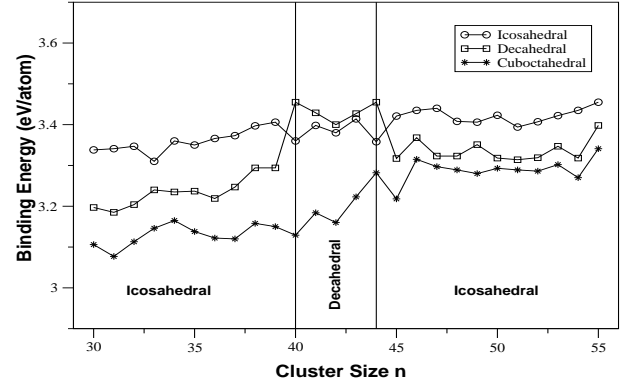


FIG. 3: Comparison of binding energies per atom as a function of cluster size n among cuboctahedral, decahedral and icosahedral structures. For the whole region most of the clusters prefer icosahedral structure. However, a local geometrical change from icosahedral to decahedral structure is found for $n = 40 - 44$.

ing energies. The LDA based ab initio calculations always over-estimate binding energies. This is a characteristic of the LDA. In the present study, TB parameters have been fitted to the ab initio LDA calculations for very small calculations [22]. It is not surprising therefore that the binding energies are over-estimated. In fact, the present results agree well with other LDA based calculations [19, 22], all of which overestimate the binding energy.

In the Fig.3, we compared binding energy per atom for cuboctahedral, decahedral and icosahedral structures for the clusters containing $n = 30 - 55$ atoms. Fig.3 shows most of the clusters in this size range have icosahedral structures. However, a local structural change occurred for $n = 40 - 44$, where the structures adopt decahedral structure rather than icosahedral one. Return to the icosahedral growth pattern is found at $n = 45$ and continues up to 55-atom cluster. From the Fig.3 it is clear that among cuboctahedral, decahedral and icosahedral structures, cuboctahedral structures are least stable than the other two.

The second difference in the binding energy may be calculated as

$$4_2E(n) = E(n+1) + E(n-1) - 2E(n); \quad (16)$$

where $E(n)$ represents the total energy for an n -atom cluster. $4_2E(n)$ represents the relative stability of an n -atom cluster with respect to its neighbors and can be directly compared to the experimental relative abundance: the peaks in $4_2E(n)$ coincide with the discontinuities in the mass spectra. These are plotted in the lower panel of Fig.2. We found three major characteristics in the Fig.2 (lower panel). Firstly, even-odd (even > odd) oscillation is found. This can be explained in terms of electron pairing in HOMOs. Even (odd) clusters have an even (odd) number of electrons and the HOMO is doubly (singly) occupied. The electron in a doubly occupied

HOMO will feel a stronger effective core potential because the electron screening is weaker for the electrons in the same orbital than for inner shell electrons. Thus the binding energy of the valence electron with an even cluster is larger than of an odd one. This even-odd alternation is prominent up to $n = 40$. Secondly, due to electronic shell or subshell closing, we found particular high peak for $n = 8; 18; 20; 34$ and 40 . Unfortunately, the present study does not show any evidence of shell closing for Cu_2 in $4_2E(n)$. Finally, the even-odd alternation is reversed for $n = 10 - 16$ with maxima at Cu_{11} , Cu_{13} and Cu_{15} , which manifests the geometrical effect and therefore there is no peak at $n = 14$ due to electronic subshell closing. Simultaneous appearance of these three features in $4_2E(n)$ demonstrates the interplay between electronic and geometrical structure, which is in agreement with the experimental study of Winter et al. [50]. They found both jellium-like electronic behaviour and icosahedral structure in copper clusters. In an experimental study of mass spectra of ionized copper clusters [10], substantial discontinuities in mass spectra at $n = 3; 9; 21; 35; 41$ for cationic and $n = 7; 19; 33; 39$ for anionic clusters as well as dramatic even-odd alternation are found. From the sudden loss in the even-odd alternation at Cu_{42} in the KRC spectrum, Winter et al. argued about the possible geometrical change there. Therefore, we conclude in the section that sudden loss in the 4_2E vs n plot (lower panel of Fig. 2) is due the structural change in that regime.

Such kind of electronic effects can not be reproduced by empirical atomistic potentials. Darby et al. [26], using the Gupta potential, found significant peaks at $n = 7, 13, 19, 23$ and 55 due to icosahedral (or polyicosahedral) geometries. In the present study, we have found a peak at $n = 13$, but not at the other sizes found by them. However, the stable structures predicted by us are the same: the lowest energy structure of Cu_7 is a pentagonal bipyramid (D_{5h} symmetry); for $n = 13$ and 55 , the structure are the first and second closed icosahedral geometries respectively. Polyicosahedral structures are found for $n = 19$ (double icosahedron) and $n = 23$ (triple icosahedron) atom clusters. As the reason, the present study shows significant high peaks at Cu_8 , Cu_{18} and Cu_{20} due to electronic shell closing effect and average peaks at Cu_{22} and Cu_{24} due to electron pairing effect. At these sizes, the electronic effects dominates over the geometrical effects and consequently the above peaks cannot be observed by Darby et al.

C. HOMO-LUMO gap energies

Besides the second difference of the cluster binding energy, a sensitive quantity to probe the stability is the highest occupied-lowest unoccupied molecular level (HOMO-LUMO) gap energy. In the case of magic clusters shell or subshell closer manifests themselves in particularly large HOMO-LUMO gap, which was previ-

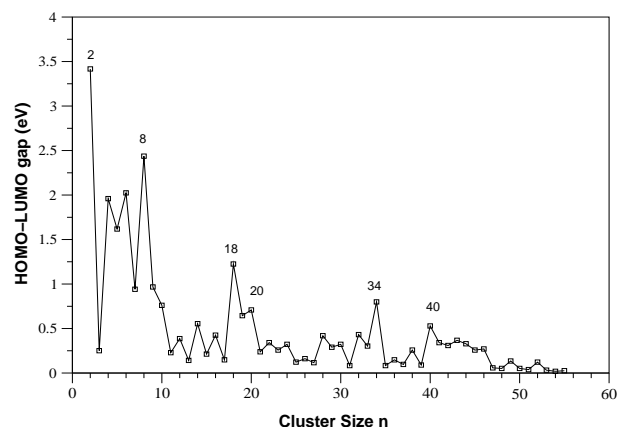


FIG. 4: Highest occupied - lowest unoccupied molecular orbital (HOMO-LUMO) gap energy vs cluster size n . Electronic shell closer at $n = 2, 8, 18, 20, 34, 40$ and even-odd alternation are observed. However, sudden loss in even-odd alternation is found around $n = 40$ due to the structural change there.

ously demonstrated experimentally [16, 55]. Calculated HOMO-LUMO gap energies are plotted in the Fig. 4, where we observed even-odd alternation due to electron pairing effect and particularly large gap for $n = 2, 8, 18, 20, 34$ and 40 due to electronic shell and subshell closing. However, sudden loss of even-odd alternation is found around $n = 40$ due to the change in the geometrical structure in that region. Winter et al. [50] also found a sudden loss in even-odd alternation in the KRC spectrum at Cu_{42} and concluded this may coincide with any possible change in the geometrical structure there. In fact, Katakuse et al. [10] observed identical behaviour in the mass spectra of sputtered copper and silver cluster ions: a dramatic loss of even-odd alternation at $n = 42$, signifying a sudden change to a geometrical structure in which stability, and abundance, is less sensitive to electron pairing. Therefore, the sudden loss in the Fig. 4 again confirms the structural change there. So, the present study correctly predicts the "magic numbers" in this regime correctly and confirms the experimental prediction: a geometrical change (icosahedron \rightarrow decahedron) is occurring around $n = 40$.

D. Ionization potentials

Within the present TB scheme, we can get a 'qualitative' description of the ionization potentials with cluster size according to Koopmans' theorem. This limitation arises mainly from the choice of the Slater-Koster (SK) TB parameters and the extent of their transferability [56], which may be improved by the proposed scaling scheme of Cohen, Mehl and Papaconstantopoulos [57]. However, our aim is to get only a qualitative description of ionization potential with cluster size. Calculated ionization potentials are plotted in the Fig. 5. In fact, we observed same pattern as it was in HOMO-LUMO gap

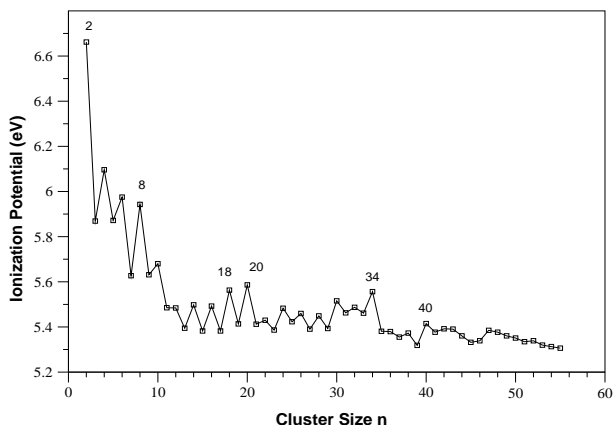


FIG. 5: Ionization potential vs cluster size n . Electronic shell closing effect and prominent even-odd alternation up to $n = 40$ are observed.

energy vs cluster size : peaks at $n = 2, 8, 18, 20, 34, 40$ and even-odd alternation due to the same reasons discussed in the Sec. IIIB. and Sec. IIIC. Sudden loss in even-odd alternation around $n = 40$ is again confirmed from the Fig.5, which is due to the geometrical change there.

IV. CONCLUSION

Using tight-binding model we calculated ground state geometries, binding energies, second differences in binding energy, HOMO-LUMO gap energies and ionization potentials for copper clusters in the size range $2 \leq n \leq 55$. We have fitted the parameters of the present TB scheme from our previous ab initio calculations [22]. For small clusters $n \leq 9$, present results show good agreement with experimental [16, 18] and theoretical [19, 20, 21, 22, 47, 48, 49] results, which allow us to go over the larger size range, $10 \leq n \leq 55$.

In the size range $10 \leq n \leq 55$ most of the clusters adopt icosahedral geometry which can be derived from the 13-atom icosahedron, the polyicosahedral 19-, 23-, and 26-atom clusters and 55-atom icosahedron, by adding or removing atoms. However, exceptions to the icosahedral growth is found around $n = 40$. A local geometrical transition is found for $n = 40-44$ -atom clus-

ters. This is in agreement with the prediction of the two experimental studies by Katakuse et al. [10] and Winter et al. [50], where they predicted that a local geometrical transition may occur at $n = 42$, though their results are not decisive about the nature of this geometrical change. Present results show that around $n = 40$ structures are changing from icosahedral to decahedral structure, where the structural sequence is decahedron-icosahedron-cuboctahedron in the decreasing order of stability. Return to the icosahedral growth is found at $n = 45$, with the sequence icosahedron-decahedron-cuboctahedron in the decreasing order of stability.

As we have fitted the parameters of the present TBMD scheme from LDA based ab initio calculations [22], calculated binding energies are in good agreement with the LDA based ab initio calculations but overestimates the same calculated from the TCID experiment [18]. In the present scheme, the "magic numbers" ($n = 2, 8, 18, 20, 34$ and 40) due to electronic shell and subshell closing are correctly reproduced in the studied regime. Second difference of binding energy, HOMO-LUMO gap energy and ionization potential show even-odd oscillatory behaviour because of electron pairing in HOMOs in agreement with experiment. However, a sudden loss in even-odd alternation is found around $n = 40$ in the variation of second difference in binding energy, HOMO-LUMO gap energy and ionization potential with cluster size. This is in agreement with the experimental studies [10, 50]. We conclude this is due to the geometrical change (icosahedron ! decahedron) around there. Present results show that electronic structure can coexist with a fixed atomic packing.

Due to lower computational expense this TBMD scheme, with parameters fitted to first-principle calculation for the smaller clusters and with an environment correction, is a very efficient technique to study larger clusters, particularly with $n \geq 10$.

Acknowledgments

This work is partially supported by the Centre for Catalytic Systems and Materials Engineering, University of Warwick, U. K. The authors are deeply grateful to S. Mukherjee and Luciano Colombo for helpful discussion.

[1] W. A. de Heer, Rev. Mod. Phys. 65, 611 (1993).
 [2] M. Brack, Rev. Mod. Phys. 65, 677 (1993).
 [3] M. Valden, X. Lai and D. W. Goodman, Science 281, 1647 (1998).
 [4] M. B. Knickelbein, Annu. Rev. Phys. Chem. 50 79 (1999).
 [5] S. H. Joo, S. J. Choi, I. Oh, J. Kwak, Z. Liu, O. Terasaki and R. Ryoo, Nature (London) 412, 169 (2001).
 [6] P. L. Hansen, J. B. Wagner, S. Helveg, J. R. Rostrup-

Nielsen, B. S. Clausen and H. Topsøe, Science 295, 2053 (2002).
 [7] C. Binns, Surf. Sci. Rep. 44, 1 (2001).
 [8] S. J. Park, T. A. Taton and C. A. Mirkin, Science 295, 1503 (2002).
 [9] D. I. Gittins, D. Bethell, D. J. Schirrin and R. J. Nicolais, Nature (London) 408, 67 (2000).
 [10] I. Katakuse, T. Ichihara, Y. Fujita, T. Matsuo, T. Sakurai and H. Matsuda Int. J. Mass Spectrom. Ion P. 67,

- 229 (1985); 74, 33 (1986).
- [11] J. Tiggelbaumer, L. Koller, K. Meiwes-Broer and A. Liebsch, *Phys. Rev. A* 48, 1749 (1993).
- [12] G. Apai, J. F. Hamilton, J. Stohr and A. Thompson, *Phys. Rev. Lett.* 43, 165 (1979).
- [13] A. Balema, E. Bemicri, P. Piccozi, A. Reale, S. Santucci, E. Burrattini and S. M. Obilio, *Surf. Sci.* 156, 206 (1985).
- [14] P. A. Montano, H. Purdum, G. K. Shenoy, T. I. Morrison and W. Schultze, *Surf. Sci.* 156, 216 (1985).
- [15] K. J. Taylor, C. L. Pettiette-Hall, O. Cheshnovsky and R. E. Smalley, *J. Chem. Phys.* 96, 3319 (1992).
- [16] J. Ho, K. M. Ervin and W. C. Lineberger, *J. Chem. Phys.* 93, 6987 (1990).
- [17] M. B. Knickelbein, *Chem. Phys. Lett.* 19, 2129 (1992).
- [18] V. A. Spasov, T. H. Lee and K. M. Ervin, *J. Chem. Phys.* 112, 1713 (2000).
- [19] C. M. Assobrio, A. Pasquarello, R. Car, *Chem. Phys. Lett.* 238, 215 (1995).
- [20] P. Calaminci, A. M. Koster, N. Russo, and D. R. Salahub, *J. Chem. Phys.* 105 9546 (1996).
- [21] H. Akeby, I. Panas, L. G. M. Pettersson, P. Seigbahn and U. Wahlgren, *J. Chem. Phys.* 94 5471 (1990).
- [22] M. K. Abir, A. Mookerjee, R. P. Datta, A. Banerjee and A. K. Bhattacharya *Int. J. Mod. Phys. B* 17, 2061 (2003).
- [23] R. P. Datta, A. Banerjee, A. Mookerjee and A. K. Bhattacharya, *Electronic Structure of Alloys, Surfaces and Clusters* ed. D. D. Sarna and A. Mookerjee (Taylor and Francis, New York) 348 (2003).
- [24] G. D'Agostino, *Philos. Mag. B* 68, 903 (1993).
- [25] R. P. Gupta, *Phys. Rev. B* 23, 6265 (1983).
- [26] S. Darby, T. V. Mortimer-Jones, R. L. Johnston and C. Roberts, *J. Chem. Phys.* 116, 1536 (2002).
- [27] M. Menon and R. E. Allen, *Phys. Rev. B* 33, 7099 (1986); 38, 6196 (1988).
- [28] M. Menon and K. R. Subbaswamy, *Phys. Rev. B* 47, 12754 (1993); 50, 11577 (1994); 51, 17952 (1996).
- [29] P. Ordejon, D. Lebedenko and M. Menon, *Phys. Rev. B* 50, 5645 (1994).
- [30] M. Menon, J. Connolly, N. Lathiotakis and A. Andriotis, *Phys. Rev. B* 50, 8903 (1994).
- [31] N. Lathiotakis, A. Andriotis, M. Menon and J. Connolly, *J. Chem. Phys.* 104, 992 (1996).
- [32] J. Zhao, Y. Luo and G. Wang, *Eur. Phys. J. D* 14, 309 (2001).
- [33] J. C. Slater and G. F. Koster, *Phys. Rev.* 94, 1498 (1954).
- [34] W. A. Harrison, *Electronic Structure and the Properties of Solids* (Dover, 1989).
- [35] N. Aslund, R. F. Barrow, W. G. Richards and D. N. Travis, *Ark. Fys.* 30 171 (1965).
- [36] D. Tománek and M. Schlüter, *Phys. Rev. B* 36, 1208 (1987).
- [37] K. P. Huber and G. Herzberg, *Molecular Spectra and Molecular Structure*, Vol. IV (Van Nostrand-Reinhold, New York, 1989).
- [38] R. P. Feynman, *Phys. Rev.* 56, 340 (1939).
- [39] L. Colombo, (Unpublished).
- [40] W. C. Swope, H. C. Anderson, P. H. Berens and K. R. Wilson, *J. Chem. Phys.* 76, 637 (1982).
- [41] M. S. Methfessel and van M. Schilfgaarde, *Phys. Rev. B* 48, 4937 (1993); *Int. J. Mod. Phys. B* 7, 262 (1993); M. S. Methfessel, van M. Schilfgaarde and M. Schärer, *Phys. Rev. Lett.* 70, 29 (1993).
- [42] D. M. Deaven and K. M. Ho, *Phys. Rev. Lett.* 75, 288 (1995); D. M. Deaven, N. T. It, J. R. Morris and K. M. Ho, *Chem. Phys. Lett.* 256, 195 (1996).
- [43] B. Hartke, *Chem. Phys. Lett.* 240, 560 (1995).
- [44] Y. H. Luo, J. J. Zhao, S. T. Qiu and G. H. Wang, *Phys. Rev. B* 59, 14903 (1999).
- [45] J. A. Niesse and H. R. Mayne, *Chem. Phys. Lett.* 261, 576 (1996); *J. Chem. Phys.* 105, 4700 (1996).
- [46] M. K. Abir, A. Mookerjee and A. K. Bhattacharya, unpublished.
- [47] C. W. Bauschlicher, Jr., S. R. Langhorne and H. Partridge, *J. Chem. Phys.* 91, 2412 (1989); C. W. Bauschlicher, Jr., *Chem. Phys. Lett.* 156, 91 (1989).
- [48] U. Lammers and G. Borstel, *Phys. Rev. B* 49, 17360 (1994).
- [49] Y. Wang, T. F. George, D. M. Lindsay and A. C. Beri, *J. Chem. Phys.* 86, 3593 (1987); D. M. Lindsay, L. Chu, Y. Wang and T. F. George, *ibid.* 87, 1685 (1987).
- [50] B. J. Winter, E. K. Parks and S. J. Riley, *J. Chem. Phys.* 94, 8618 (1991).
- [51] S. Valkealahti and M. Manninen, *Phys. Rev. B* 45, 9459 (1992).
- [52] Y. O. B. Christensen and K. W. Jacobsen, *J. Phys.: Condens. Matter* 5, 5591 (1993).
- [53] O. B. Christensen, K. W. Jacobsen, J. K. Nørskov and M. Manninen, *Phys. Rev. Lett.* 66, 2219 (1991).
- [54] Even a small variation in the parameters (in particular parameter q) in the Gupta potential can lead to changes in the global minimum. see K. Michaelian, N. Rendon and I. L. Garzon, *Phys. Rev. B* 60, 2000 (1999).
- [55] C. L. Pettiette, S. H. Yang, M. J. Craycraft, J. Conceicao, R. T. Laaksonen, O. Cheshnovsky and R. E. Smalley, *J. Chem. Phys.* 88, 5377 (1988).
- [56] The set of SK-TB parameters in this scheme implies that within the Koopmans' theorem, ionization potentials are approximately equal to the on-site energy $E_s = E_d$, which is usually much higher than highest occupied s-orbital energy of the free atom. A constant shift is made in plotting of the Fig. 5. See Ref. [31].
- [57] R. E. Cohen, H. J. Mehl and D. A. Papaconstantopoulos, *Phys. Rev. B* 50, 14694, (1994).